Real-Time Wavelet-Based Distribution Systems Disturbances Detection

Rodrigo de A. Coelho, Karcius M. C. Dantas, Érica M. Lima, Núbia S. D. Brito, Kézia de V. O. Dantas, Raquel Zacarias

***Abstract*—Distribution feeders are prone to different types of events, such as disturbances and faults. Since these events are both unwanted and unexpected, their detection is essential for prompt system restoration, ensuring its reliability. This paper proposes the use of a power component, defined for non-sinusoidal conditions, as a disturbance detection index, which is estimated using the real-time stationary discrete wavelet packet transform. The proposed method analyzes the voltage and current of each phase separately, which are acquired at a single upstream measurement point, the substation. The performance and effectiveness of the proposed method are evaluated using events simulated in a test system based on a real distribution network. The results attest that the proposed method is suitable for detecting non-stationary disturbances.**

***Keywords*—Distribution networks, disturbance signals detection, non-stationary waveforms, wavelet transform.**

I. Introduction

ELECTRICAL power systems are susceptible to disturbances and events that can reduce service continuity. In this context, it is critical for power system operators to have accurate information to assess system conditions. Once these disturbances are non-stationary, such as transients induced by switching events, the approach to detect them must be appropriate to characterize time instants associated with its occurrence.

A typical approach to disturbances detection comprises analyzing the root-mean-square (RMS) value of voltage and/or current signals [1], [2]. However, since the fundamental component is dominant in power system signals, when a disturbance effect reverberates only in harmonics, the RMS value may not be sufficient to detect a disturbance.

The signal frequency content is also used to characterize disturbances, which is usually obtained through the Fourier transform (FT) [3]. Nevertheless, the FT is not suitable for analyzing non-stationary signals. For these conditions, transforms such as short-time Fourier transform (STFT), wavelet transform (WT), and Stockwell transform (ST) are commonly applied to signal analysis [4].

The WT stands out in the analysis of disturbances caused by common power system events. This transform, along with its variants, is often studied for the detection, identification, and temporal localization of power quality disturbances.

Several works [5], [6], [7] highlight the use of conventional WT to diagnose variations in the signal's frequency and amplitude, as well as the possibility of quickly identifying disturbances. In [5], for instance, WT is adopted to detect and identify voltage sag and swell, interruptions, transients, and the presence of harmonics. WT variations such as orthogonal and packet [8], [9] are used for both detection and temporal location of disturbances, and also to provide a discriminating indicator for power quality evaluation.

Complex Gaussian WT is applied in [10] to detect voltage variations, pulse interference, instantaneous interruption, and frequency fluctuations, as well as locate them in time. The author adopted the phase difference between these signals and a pure sinusoidal one as a detection and identification parameter. Ref. [11], in turn, proposed an improvement for WT using coefficients that approach boundary distortions, to avoid the influence of the mother wavelet's choice. The author analyzes signals from high and low impedance faults, among other power quality disturbances, comprising the distribution and transmission system. However, power distribution systems often have a low amount of equipment for signals monitoring, which may discourage the application of techniques that require a high level of signal supervision.

In this paper, a method for disturbance detection in distribution systems is proposed. The signals parameters are extracted by using the real-time version of the stationary discrete wavelet packet transform (SDWPT), which is a prominent technique for analyzing non-stationary signals. From time-frequency signals characterization, power components appropriate for non-sinusoidal conditions are calculated. This work proposes the usage of one of these power component as disturbance detection index, which has a behavior suitable to indicate several events in power systems, especially at distribution level.

The proposed method is advantageous because it analyzes the voltage and current phase signals acquired at a single upstream measurement point, the substation. Furthermore, the parameters here presented show potential as an indicator for detection and temporal location of disturbances, such as feeder and transformer energizing, capacitor banks switching, and

This work was supported by National Council for Scientific and Technological Development (CNPq), grant number 167379/2018-6, and by Agência Nacional de Energia Elétrica R&D Program (Light SA/UEPB/UFCG/PaqTc-PB), grant number PD-00382-0132/2020.

R. A. Coelho is with Graduate Studies Program in Electrical Engineering, Federal University of Campina Grande (UFCG), Campina Grande-PB, Brazil (e-mail of corresponding author: rodrigo.almeida@ee.ufcg.edu.br). K. M. C. Dantas and N. S. D. Brito are with Electrical Engineering Department of Federal University of Campina Grande (DEE/UFCG), Campina Grande-PB, Brazil (e-mails: {nubia; karcius}@dee.ufcg.edu.br). E. M. Lima is with Engineering Department of Federal University of the Semi-arid Region (UFERSA), Caraúbas-RN, Brazil (e-mail: erica.lima@ufersa.edu.br). K. V. O. Dantas is with Department of Computer Science of State University of Paraíba, Campina Grande-PB, Brazil (e-mail: kezia.vasconcelos@servidor.uepb.edu.br). R. Zacarias is with Light SA, Rio de Janeiro-RJ, Brazil (e-mail: raquel.souza@light.com.br).

Paper submitted to the International Conference on Power Systems Transients (IPST2023) in Thessaloniki, Greece, June 12-15, 2023.

low and high impedance faults.

II. Stationary Discrete Wavelet Packet Transform (SDWPT)

The wavelet transform provides a local representation in both time and frequency domains of a given signal by a prototype function called the mother wavelet with adaptable scaling properties [12]. The discrete wavelet transform (DWT) performs a signal decomposition into scaling and wavelet coefficients by using low- and high-pass digital filters respectively, at various decomposition levels [13]. Thus, each coefficient represents a given band of the frequency spectrum.

The wavelet packet algorithms can be interpreted as a WT generalization, where both scaling and wavelet coefficients are used as input in a given decomposition level [14], as depicted in Fig. 1. By using the SDWPT, the coefficients present a uniform frequency bandwidth, which can be useful to properly isolate frequency ranges within the spectrum analyzed [15], allowing to evaluate frequency components separately [16].

The SDWPT coefficients, at the m decomposition level, are defined as [17]:

$$x_m^{2p}[k] = \frac{1}{\sqrt{2}} \sum_{l=-\infty}^{\infty} h_\varphi[l] x_{m-1}^p[k-l], \tag{1}$$

$$x_m^{2p+1}[k] = \frac{1}{\sqrt{2}} \sum_{l=-\infty}^{\infty} h_\psi[l] x_{m-1}^p[k-l], \tag{2}$$

where x_0^0 is the original signal, p is the node number ($0 \leq p \leq 2^{m-1}-1$, $p \in \mathbb{N}$), $h_\varphi[l]$ and $h_\psi[l]$ are the low- (scaling) and high-pass (wavelet) filters, respectively.

The scaling and wavelet filters are associated to a mother wavelet and satisfy the following properties [18]:

$$\sum_{l=1}^{L} h_\varphi[l] = \sqrt{2}, \quad \sum_{l=1}^{L} h_\varphi^2[l] = 1, \quad \sum_{l=1}^{L} h_\varphi[l] h_\psi[l] = 0, \tag{3}$$

$$\sum_{l=1}^{L} h_\psi[l] = 0, \quad \sum_{l=1}^{L} h_\psi^2[l] = 1, \quad \sum_{l=1}^{L} h_\psi[l] h_\varphi[l] = 0, \tag{4}$$

where L denotes the length of the filter. Furthermore, the scaling and wavelet filters satisfy a quadrature mirror filter (QMF) relationship, namely

$$h_\varphi[l] = (-1)^{l+1} h_\psi[L-l-1], \tag{5}$$

$$h_\psi[l] = (-1)^{l} h_\varphi[L-l-1]. \tag{6}$$

Assuming that h_φ and h_ψ are finite impulse response (FIR) quadrature mirror filters, the real-time SDWPT (RT-SDWPT) decomposition coefficients can be obtained by convolving the input signal with these filters [17]. According to [19], the RT-SDWPT coefficients are

$$x_m^{2p}[k] = \frac{1}{\sqrt{2}} \sum_{l=0}^{L-1} h_\varphi[l] x_{m-1}^p[k+l-L+1], \tag{7}$$

$$x_m^{2p+1}[k] = \frac{1}{\sqrt{2}} \sum_{l=0}^{L-1} h_\psi[l] x_{m-1}^p[k+l-L+1]. \tag{8}$$

The RT-SDWPT coefficients are useful for both stationary and non-stationary signal characterization. Since the actual sample only depends on the previous samples, the RT-SDWPT improves the signal analysis, mainly for estimating time instants associated with the power system disturbances occurrence.

III. Methodology for disturbance detection

A. Power calculation

The basis for the use of the WT for power and RMS measurements was demonstrated by [20], which was improved by several works over years [21], [22], [23]. One of these methods proposes the use of RT-SDWPT for power measurement purposes [19], according to which the RMS value of a given signal $x[k]$ at q node (or frequency subband) is:

$$X_m^q[k] = \sqrt{\frac{1}{2W} \sum_{w=k-W+1}^{k} \sum_{l=0}^{L-1} \left(x_m^q[w-l]\right)^2}, \tag{9}$$

where W denotes the window length and $0 \leq q \leq 2^m - 1$ ($q \in \mathbb{N}$).

Hence, the RMS value of the $x[k]$ signal at kth sample is given by

$$X[k] = \sqrt{\sum_{q=0}^{2^m-1} \left(X_m^q[k]\right)^2} \tag{10}$$

where $X = V$ and $X = I$ for voltage and current signals, respectively.

Regardless of the signals condition, the active power corresponds to the average value of the instantaneous power, whereas the apparent power is obtained by the product of voltage and current RMS values. These powers can be estimated by using the RT-SDWPT as follows [19]:

$$\begin{aligned} P[k] &= \sum_{q=0}^{2^m-1} \frac{1}{2W} \sum_{w=k-W+1}^{k} \sum_{l=0}^{L-1} v_m^q[w-l] i_m^q[w-l] \\ &= \sum_{q=0}^{2^m-1} P_m^q[k] \quad \text{(W)}, \end{aligned} \tag{11}$$

$$\begin{aligned} S[k] &= V[k] I[k] \\ &= \sqrt{\sum_{q=0}^{2^m-1} \left(V_m^q[k]\right)^2} \sqrt{\sum_{q=0}^{2^m-1} \left(I_m^q[k]\right)^2} \\ &= \sqrt{\sum_{q=0}^{2^m-1} \left(V_m^q[k]\right)^2 \left(I_m^q[k]\right)^2} \\ &= \sqrt{\sum_{q=0}^{2^m-1} \left(S_m^q[k]\right)^2} \quad \text{(VA)}, \end{aligned} \tag{12}$$

where $P_m^q[k]$ and $S_m^q[k]$ are the active and apparent powers at q node, respectively, whereas $P[k]$ and $S[k]$ denotes the active and apparent powers of voltage and current pair, respectively.

By using the WT approach to analyze signals, an inherent effect is the inter-band spectrum leakage, which commits the frequency representation of each coefficient [24]. This occurs because a given coefficient contains information about the

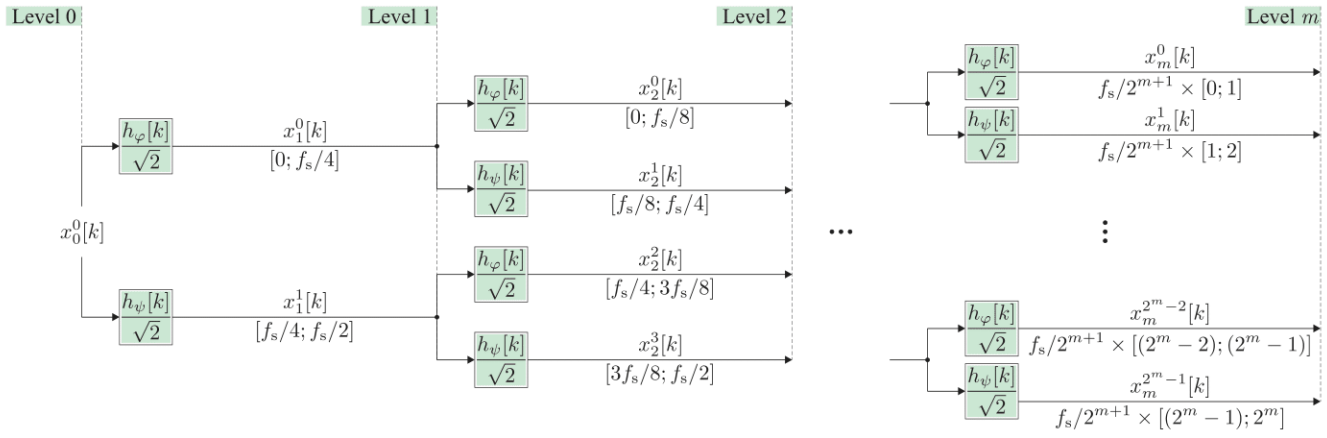

Fig. 1. m-level SDWPT decomposition tree.

frequencies located near the outskirts of this ideal frequency range. Although it cannot be completely mitigated, this effect can be minimized by adopting longer mother wavelets. However, once the wavelet answer is slower for long mother wavelets [25], [26], this type of wavelet function is not appropriate for real-time analysis.

In [27] was proposed an apparent power decomposition in four terms, namely active, reactive, diffuse and residual powers. The reactive power is related to phase deviation between voltage and current, the diffuse power refers to an energy dissipated in circuit resistance, and the residual power quantifies the power portion associated with frequency components contained only in current signal. As previously related, the WT decomposition has an inherent spectrum leakage, which can compromise the residual power representation. For this reason, this work adopts an apparent power decomposition in terms only of active, $P[k]$, reactive, $Q[k]$, and diffuse, $D[k]$, powers, namely:

$$S^2[k] = P^2[k] + Q^2[k] + D^2[k]. \tag{13}$$

According to [27], the value of displacement angle between voltage and current is mandatory for $Q[k]$ and $D[k]$ calculation. Despite the WT does not provide directly the phase angle information, this parameter can be artificially estimated via WT approach from P and S relationship as proposed in [28], [29]. Based on $P_m^q[k]$ and $S_m^q[k]$, the phase shift between voltage and current of each q node can be estimated as

$$\phi_m^q[k] = \cos^{-1}\left(\frac{P_m^q[k]}{S_m^q[k]}\right). \tag{14}$$

Thus, the reactive and diffuse powers can be estimated via RT-SDWPT as follows:

$$Q[k] = V[k]\sqrt{\sum_{q=0}^{2^m-1}\left(I_m^q[k]\sin\left(\phi_m^q[k]\right)\right)^2} \quad \text{(VA)}, \tag{15}$$

$$D[k] = \left[\sum_{0\le a<b\le 2^m-1}\left(V_m^b[k]I_m^a[k]\cos\left(\phi_m^a[k]\right) - V_m^a[k]I_m^b[k]\cos\left(\phi_m^b[k]\right)\right)^2\right]^{\frac{1}{2}} \quad \text{(VA)}. \tag{16}$$

Despite having a similar formulation to distortion power proposed by Budeanu [30], the diffuse power computes only the power portion associated with resistive elements without contributing to active power [27]. As diffuse power is associated with energy dissipated without effectively realizing work, it constitutes an indicator of the occurrence of events in the power system. Furthermore, as related in (16), this power component contains the contribution of all frequency components. For this reason, it is proposed that this power be used as a power system disturbance detection index.

B. RT-SDWPT parameters

Typically, odd harmonics are dominant in both supply voltage and load currents [31]. For this reason, it is necessary to perform the WT decomposition so that both fundamental component and odd harmonics are located in the center of each frequency band associated with RT-SDWPT coefficients. Therefore, since the fundamental frequency is f_1, each coefficient ideally contains the frequency spectrum spaced in $2f_1$.

According to Fig. 1, the frequency range of each coefficient is related with the sampling rate (f_s) and the number of decomposition levels (m) as follows

$$\frac{f_s}{2^{m+1}} = 2f_1. \tag{17}$$

As the adopted sampling rate is 15360 Hz and the fundamental frequency is 60 Hz, solving (17) results in $m = 6$. Therefore, six decomposition levels are necessary to adequately isolate the aforementioned frequency components, as summarized in Table I.

Another parameter with direct influence in the wavelet-based analysis is the window length, W. Different window lengths were evaluated, where the most accurate results were obtained by using a half-cycle window. For this reason, $W = 128$ was adopted.

Furthermore, the adopted mother wavelet was db4 (here, db$L$ refers to a wavelet of Daubechies family [32] with L length). This wavelet family is appropriated to analyze the power system signals and has been widely used for this purpose [33].

TABLE I
ASSOCIATION OF RT-SDWPT COEFFICIENTS WITH FREQUENCY COMPONENTS

RT-SDWPT coefficient	Frequency range (Hz)	Frequency component located at center of bandwidth
$x_6^0[k]$	[0; 120]	1st (60 Hz)
$x_6^1[k]$	[120; 240]	3rd (180 Hz)
$x_6^2[k]$	[240; 360]	5th (300 Hz)
⋮	⋮	⋮
$x_6^{63}[k]$	[7560; 7680]	127th (7620 Hz)

C. Test system

Aiming to ensure the applicability of the proposed methodology through simulations, a real 13.8 kV distribution network from a Brazilian utility was simulated and used as test system. The single-line diagram is presented in Fig. 2. The test system includes 90 buses, an average power factor of 0.955, and linear and non-linear loads [34]. All data on the electrical and spatial characteristics, as well as the loads distributed along the transformers, were provided by the utility.

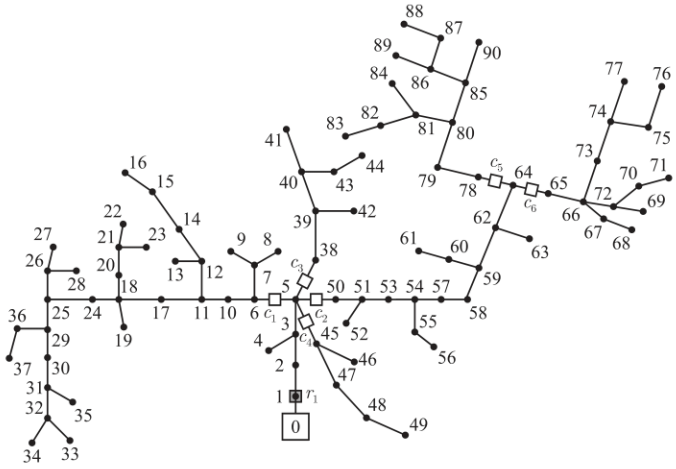

Fig. 2. Test system: single-line diagram.

D. Disturbances simulation

The proposed method was validated considering five common events in distribution networks: feeder energizing (FE), capacitor banks switching (CBS), transformer energizing (TE), high-impedance fault (HIF), and low-impedance faults (LIF). All disturbances were simulated on ATP (Alternative Transients Program) and applied to 18 different locations of the test system, which were chosen to cover the various sections of the feeder.

The feeder energizing was simulated by the insertion of a common switch between two buses of each location in the system. The capacitor banks switching was represented by a 1.8 Mvar bank provided by the local utility. As for low impedance faults, only single-phase to the ground was adopted since it is the most frequent event in a distribution network. The fault resistance was chosen to be 10 Ω. The high impedance faults were simulated considering the two-resistance and two time-controlled switches proposed by [35], which is able to emulate the different and stochastic aspects of this type of fault, such as: non-linearity, asymmetry, build-up, shoulder, and intermittence.

IV. RESULTS ANALYSIS

A. Capacitor bank switching (CBS)

Fig. 3 depicts the results of the CBS scenario on bus 4.

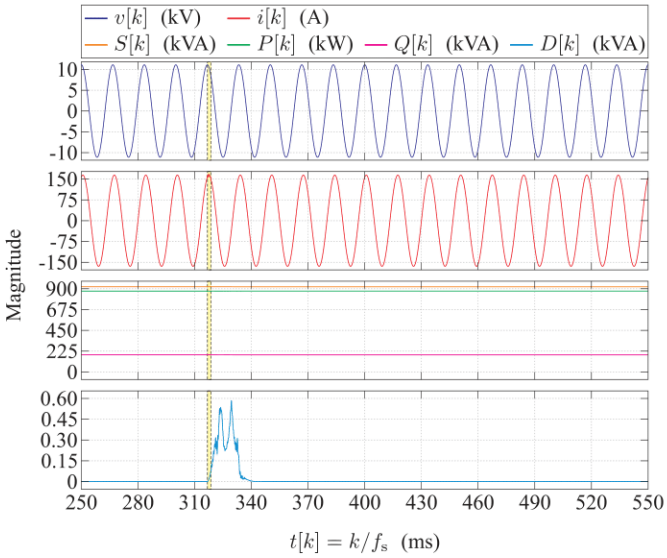

Fig. 3. CBS on bus 90: results.

Since voltage and current are monitored at the substation level, this type of event does not cause a significant change in voltage and current waveforms, as shown in Fig. 3. As a consequence, the primary power quantities, namely apparent, active and reactive powers, do not present an expressive variation. On the other hand, the diffuse power has a significant variation after disturbance occurrence. Despite having low magnitude, a portion of frequency components is inserted in the current signal at this type of event, reverberating mainly in $D[k]$. Hence, the sudden change in $D[k]$ at time instant of the event evince that this quantity is appropriate to characterize an occurrence in the power system, i.e., to detect a disturbance.

B. Feeder energizing (FE)

Fig. 4 presents the results from a FE on bus 47 of the test system.

According to Fig. 4, this type of event had a slight effect on the voltage and current signals acquired at the substation. This fact is also indicated by the small variation in $S[k]$, $P[k]$, and $Q[k]$. In contrast, the diffuse power presents a significant variation after the event, which is sufficient to detect this type of disturbance. Moreover, once the energized feeder has non-linear loads, $D[k]$ is not null after the disturbance occurrence.

C. Transformer energizing (TE)

Fig. 5 depicts the voltage and current signals as well as the estimated powers for a TE on bus 4.

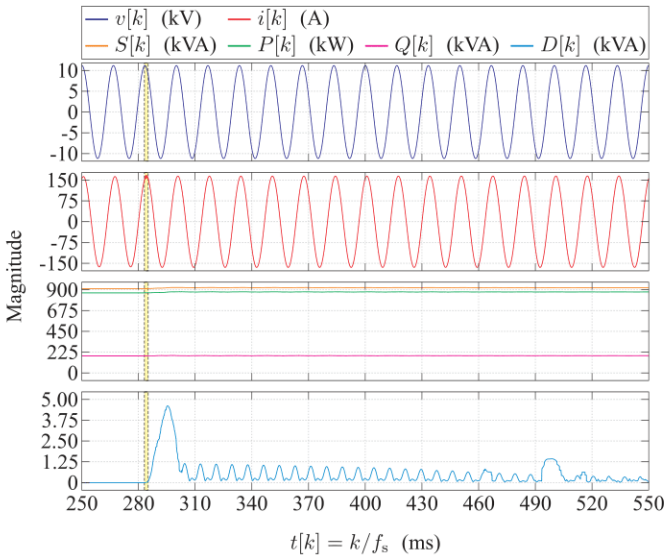

Fig. 4. FE on bus 47: results.

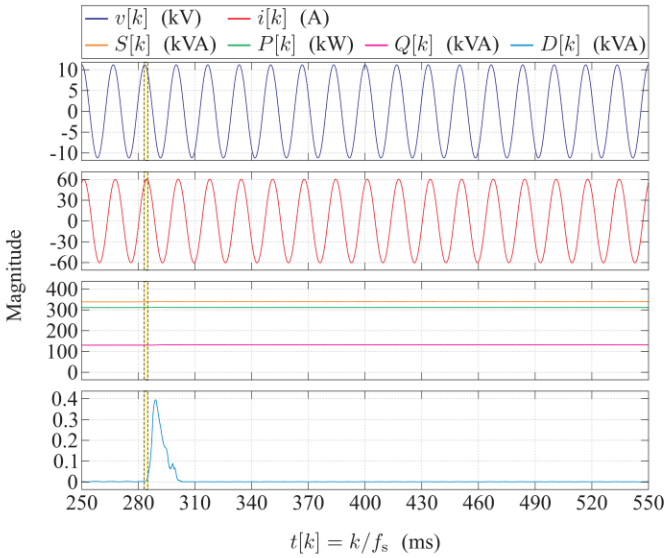

Fig. 5. TE on bus 4: results.

As represented in Fig. 5, the transient caused by this type of event does not stand out in the voltage and current signals, as they are acquired at the substation. Only the diffuse power shows a significant variation after the occurrence of the disturbance, with a peak that characterizes the occurrence of the event. Thus, $D[k]$ is appropriate for detecting this type of event.

D. High-impedance fault (HIF)

Fig. 6 illustrates the results of a HIF occurrence on bus 4 of the test system.

The peculiar characteristics of this type of fault lead to some unique distortions on current waveforms, as shown in Fig. 6. Different from previous events, apparent, active, and reactive powers also present significant variations after the disturbance occurrence. Even so, the most distinctive variation

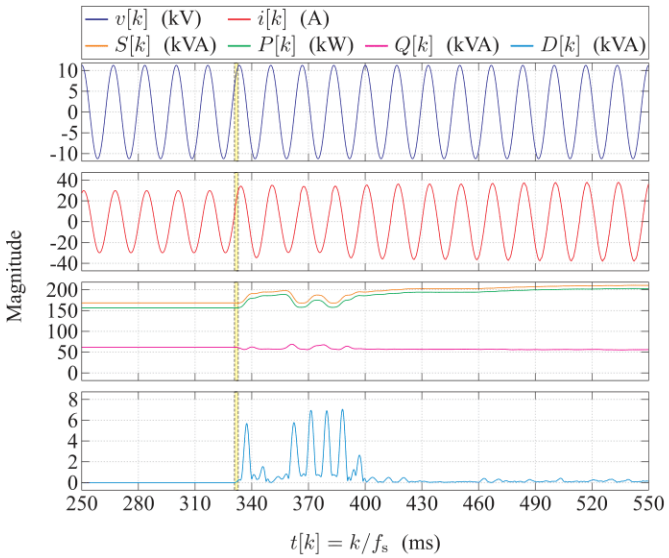

Fig. 6. HIF on bus 4: results.

was presented in $D[k]$, which retains an appropriate behavior to indicate the fault.

Moreover, the fact that $D[k]$ holds a distinctive behavior within a larger period of time, combined with the variations of $S[k]$, $P[k]$, and $Q[k]$, which were not observed in other events, suggests the possibility of using this power estimation as a proper index for both detection and selectivity, avoiding misoperation of the protection system in events such as the ones here tested.

E. Low-impedance fault (LIF)

Fig. 7 depicts the voltage and current signals and the obtained results for a LIF that occurred on bus 10 of the test system.

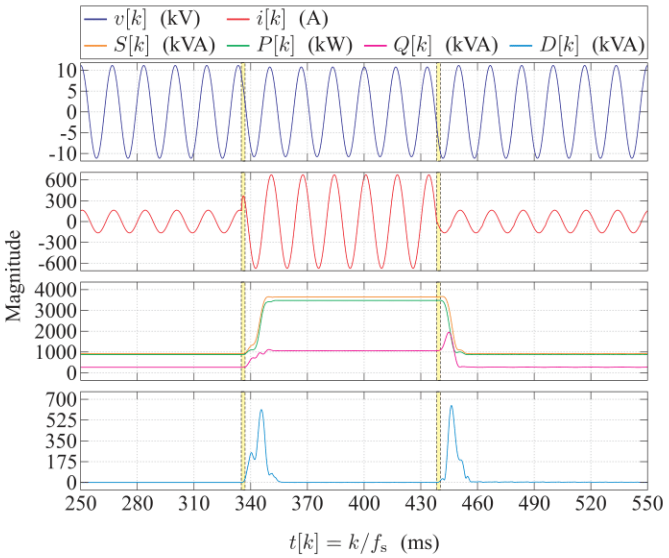

Fig. 7. LIF on bus 10: results.

According to Fig. 7, notably, all power quantities present a sudden variation at time instants for the beginning and

end of the fault. The diffuse power conserves its behavior of an abrupt peak during the occurrence of disturbance and then returns to its initial level. Whereas apparent, active, and reactive powers present a higher level throughout the event, diffuse power reaches its peaks at the beginning and at the end of the low-impedance fault, delimitating its duration. This fact is important because a simple alteration in the system loading would entail a change in $S[k]$, $P[k]$, and $Q[k]$. Therefore, this distinctive characteristic of the diffuse power can be adopted to power quality studies, evaluating the duration of disturbances and distinguishing this type of event from alterations on the system loading.

F. Effect of mother wavelet choice

It is well known that long mother wavelets provide filters with a frequency response closer to ideal. Thus, mother wavelets with higher vanishing moments provide a more appropriate frequency representation in a wavelet-based analysis. However, notably for a high number of decomposition levels, long mother wavelets represent a large computational burden.

To evaluate the mother wavelet choice effect, $D[k]$ was estimated by using a set of nine wavelet functions of the Daubechies family, namely db4, db6, db8, db10, db12, db14, db16, db18, and db20. The adopted test scenario was TE, previously presented in Sec. IV-C. The obtained results are depicted in Fig. 8.

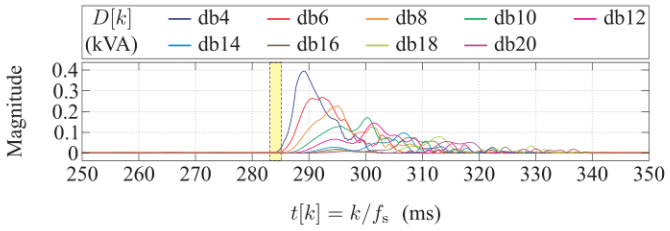

Fig. 8. TE on bus 4: effect of mother wavelet in $D[k]$ estimation.

According to Fig. 8, the obtained results by using the db4 function present a peak with a lower delay than the other mother wavelets, which is a desirable feature for real-time applications. That is, the longer the mother wavelet, the greater the delay for disturbance detection. Therefore, despite long mother wavelets providing a more accurate representation of signals, its wavelet answer is slow, which can be unsuitable for detecting power system events.

V. Comparison with other techniques

The proposed methodology was compared to other two similar techniques for detecting disturbances in power systems, namely the Stockwell transform, and the wavelet coefficients energy.

A. Wavelet-based approach

A common methodology to analyzing power systems transients using the wavelet transform is based on spectral energy. From Parseval's theorem [36], the signal energy is equal to the sum of the energy of the RT-SDWPT coefficients at the different decomposition levels:

$$\mathcal{E} = \sum_{k=1}^{N} \left|x_0^0[k]\right|^2 = \sum_{\xi=0}^{2^{m-1}} \sum_{k=1}^{N} \left|x_m^\xi[k]\right|^2, \tag{18}$$

where N denotes the size of the input signal.

However, based on (18) it is not possible to identify the energy associated with each frequency component of a given signal. To overcome this issue, as presented in [37], [38], [11], the energy can be calculated in a specific section of the coefficients using a signal sliding window. Thus, the spectral energy of a given coefficient $x_m^\xi[k]$ is computed at sample k taking into account the number of samples equivalent to the window length, that is [37],

$$\mathcal{E}_{x,m}^\xi[k] = \begin{cases} \sum_{y=1}^{W_k} x_m^\xi[y]^2, & \text{if} \quad 1 \le k \le W_k, \\ \sum_{y=k-W_k}^{k} x_m^\xi[y]^2, & \text{if} \quad W_k < k \le N, \end{cases} \tag{19}$$

where W_k denotes the window length. In this paper, $W_k = W$.

Since transients reverberate mainly in the current signal, the energy analysis will be restricted to $i[k]$, thus,

$$\mathcal{I}_1[k] = \mathcal{E}_{i,m}^0[k], \qquad \mathcal{I}_h[k] = \sum_{\xi=1}^{2^{m-1}} \mathcal{E}_{i,m}^\xi[k], \tag{20}$$

where $\mathcal{I}_1[k]$ quantifies the spectral energy associated to fundamental frequency, whereas $\mathcal{I}_h[k]$ computes the energy related to other frequency components. During a disturbance, it is expected a sudden change in $\mathcal{I}_h[k]$, whilst $\mathcal{I}_1[k]$ does not vary significantly.

Fig. 9 depicts the comparison between the proposed methodology with the wavelet coefficients energy technique for the CBS scenario. Note that wavelet coefficients energy was normalized with average values during the steady state ($\mathcal{I}_1'$ for $\mathcal{I}_1[k]$, and $\mathcal{I}_h'$ for $\mathcal{I}_h[k]$).

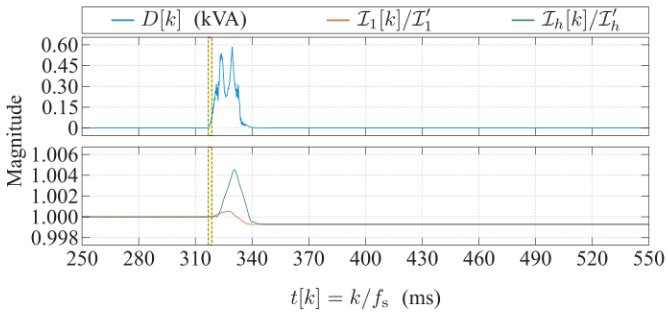

Fig. 9. CBS on bus 90: comparison between $D[k]$, $\mathcal{I}_1[k]$, and $\mathcal{I}_h[k]$ signatures.

As shown in Fig. 9, both $D[k]$ and $\mathcal{I}_h[k]$ have an abrupt variation after the disturbance, being sufficient to detect its occurrence. On the other hand, $\mathcal{I}_1[k]$ does not present a significant change after the disturbance. However, this behavior does not occur for all disturbances analyzed in this paper, as presented below.

The comparison between the proposed methodology and the wavelet coefficients energy technique for FE, TE, and HIF scenarios is depicted in Fig. 10.

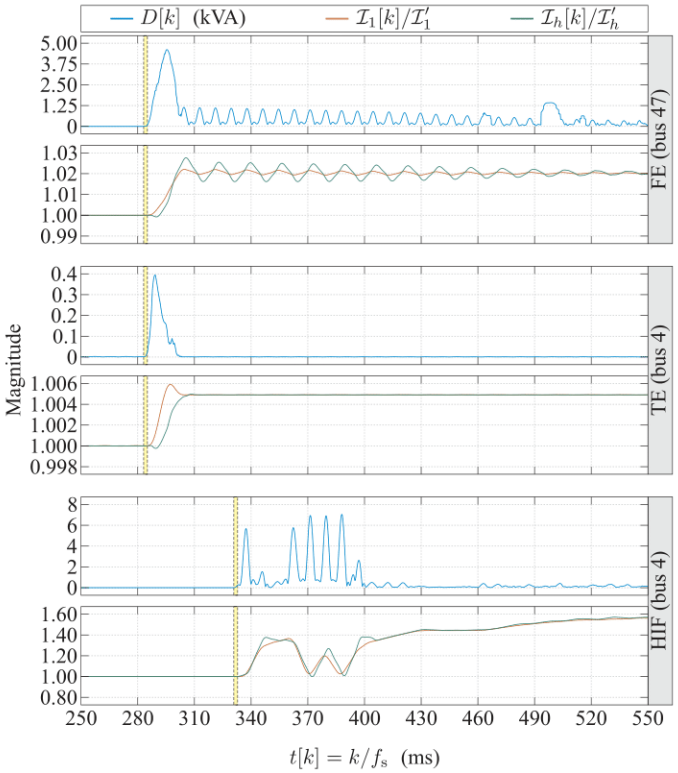

Fig. 10. FE on bus 47, TE on bus 4, and HIF on bus 4: comparison between $D[k]$, $\mathcal{I}_1[k]$, and $\mathcal{I}_h[k]$ signatures.

According to Fig. 10, after disturbances, both $\mathcal{I}_1[k]$ and $\mathcal{I}_h[k]$ vary significantly with respect to their steady-state values. That is, it is not possible to distinguish if the variation is due to a disturbance or a common occurrence in the system, such as a change in system loading. This is because the signals are measured at the substation and, therefore, represent the entire system behavior. Therefore, under these conditions, methods whose detection is based on the energy of the wavelet coefficients may not provide adequate results. On the other hand, in both cases, the diffuse power presented a signature appropriate to detect disturbances. Thereby, the proposed methodology is advantageous for supervising power systems with a low monitoring level.

B. Stockwell transform-based approach

The Stockwell transform represents an extension of the WT [39], which characteristics are appropriate for providing a classification for low-frequency short-duration disturbances and high-frequency transients [40]. The discrete Stockwell transform (DST) has been applied to several power quality studies [41], including power calculation [27], evincing its relevance for non-stationary signals analysis.

To compare the RT-SDWPT- and DST-based approaches for estimating $D[k]$ the low-impedance fault scenario was adopted, as depicted in Fig. 11.

Comparing the RT-SDWPT and the DST results for diffuse power estimation, it is evident that the measurement via

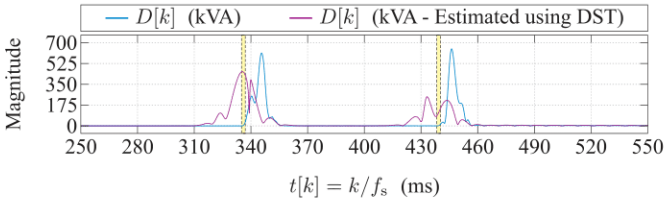

Fig. 11. LIF on bus 10 (diffuse power): comparison between RT-SDWPT and DST results.

RT-SDWPT varies only after the disturbance occurrence. On the other hand, the result from DST presents variations in time instants prior to the disturbance, which is an effect of the characteristic of the DST window. This behavior constitutes an advantage for the application of RT-SDWPT since current samples depend only on previous ones, not on future samples. Therefore, for detection purposes, the RT-SDWPT is more suitable than the DST.

VI. Conclusions

This paper proposed the use of a power component for the identification of disturbances in distribution systems. The diffuse power, which is estimated using the RT-SDWPT, was used as a disturbance detection index and proved to be appropriate to characterize several common events in distribution networks.

Five different events were simulated and analyzed: capacitor bank switching, transformer energizing, feeder energizing, and high- and low-impedance faults. The identification and characterization of these disturbances are crucial to improve power quality diagnosis as well as to assist the overcurrent protection devices in the detection of particularly worrisome disturbances such as high impedance faults.

Results show that the diffuse power behavior indicates the presence of a disturbance, presenting an abrupt peak due to its occurrence. This behavior was observed in all events analyzed in this work, and, depending on the disturbance, this quantity returns to its initial level. This power component showed potential as a duration indicator for power quality disturbances. Moreover, the diffuse power combined with other components behaves as a possible index for detecting and distinguishing high-impedance faults. Nonetheless, it is emphasized that additional tests must be performed to validate this hypothesis.

The performance of RT-SDWPT was compared to the DST-based method and wavelet coefficient energy approach. Results showed that the diffuse power estimated via RT-SDWPT is more appropriate for disturbance detection than the one calculated via DST. Furthermore, as voltage and current signals are acquired at the substation, the proposed methodology presents results more appropriate than the ones obtained by using the wavelet coefficient energy technique for disturbance detection.

Acknowledgments

This work was supported by National Council for Scientific and Technological Development, grant number

167379/2018-6, and by Agência Nacional de Energia Elétrica R&D Program (Light SA/UEPB/UFCG/PaqTc-PB), grant number PD-00382-0132/2020.

REFERENCES

[1] D. Macii and D. Petri, "Fast detection of rapid voltage change events through dynamic RMS voltage tracking," in *2018 IEEE International Instrumentation and Measurement Technology Conference (I2MTC)*, 2018, pp. 1–6.

[2] Y. Ma, Q. Li, H. Chen, H. Li, and Y. Lei, "Voltage Transient Disturbance Detection Based on the RMS Values of Segmented Differential Waveforms," *IEEE Access*, vol. 9, pp. 144 514–144 529, 2021.

[3] G. W. Chang, C. I. Chen, Y. J. Liu, and M. C. Wu, "Measuring power system harmonics and interharmonics by an improved fast Fourier transform-based algorithm," *IET Generation Transmission & Distribution*, vol. 2, pp. 192–201, 2008.

[4] R. Kumar, B. Singh, D. T. Shahani, A. Chandra, and K. Al-Haddad, "Recognition of Power-Quality Disturbances Using S-Transform-Based ANN Classifier and Rule-Based Decision Tree," *IEEE Transactions on Industry Applications*, vol. 51, no. 2, pp. 1249–1258, 2015.

[5] F. Z. Dekhandji, "Detection of power quality disturbances using discrete wavelet transform," in *2017 5th International Conference on Electrical Engineering - Boumerdes (ICEE-B)*, 2017, pp. 1–5.

[6] S. Upadhyaya and S. Mohanty, "Power Quality disturbance detection using Wavelet based signal processing," in *2013 Annual IEEE India Conference (INDICON)*, 2013, pp. 1–6.

[7] B. Eristi, O. Yildirim, H. Eristi, and Y. Demir, "A real-time power quality disturbance detection system based on the wavelet transform," in *2016 51st International Universities Power Engineering Conference (UPEC)*, 2016, pp. 1–5.

[8] L. Liu and Z. Zeng, "The detection and location of power quality disturbances based on orthogonal wavelet packet transform," in *2008 Third International Conference on Electric Utility Deregulation and Restructuring and Power Technologies*, 2008, pp. 1831–1835.

[9] A. J. Ustariz, E. A. C. Plata, and H. E. Tacca, "New Deviation Factor of Power Quality using Tensor Analysis and Wavelet Packet Transform," in *International Conference on Power Systems Transients (IPST2011)*, June 2011, pp. 1–6.

[10] G. Jing, "The phase difference method for power quality disturbance signals detection based on complex wavelet transform," in *2009 International Conference on Energy and Environment Technology*, vol. 2, 2009, pp. 348–351.

[11] F. B. Costa, "Boundary Wavelet Coefficients for Real-Time Detection of Transients Induced by Faults and Power-Quality Disturbances," *IEEE Transactions on Power Delivery*, vol. 29, no. 6, pp. 2674–2687, 2014.

[12] T. B. Littler and D. J. Morrow, "Wavelets for the analysis and compression of power system disturbances," *IEEE Transactions on Power Delivery*, vol. 14, pp. 358–364, 1999.

[13] S. G. Mallat, "A theory for multiresolution signal decomposition: the wavelet representation," *IEEE Transactions on Pattern Analysis and Machine Intelligence*, vol. 11, no. 7, pp. 674–693, July 1989.

[14] A. Jensen and A. la Cour-Harbo, *Ripples in Mathematics: The Discrete Wavelet Transform*, 1st ed. Springer-Verlag Berlin Heidelberg, 2001.

[15] H. M. G. C. Branco, D. Barbosa, M. Oleskovicz, and D. V. Coury, "Classification of events in power transformers using wavelet packet transform and fuzzy logic," *Journal of Control, Automation and Electrical Systems*, vol. 24, pp. 300–311, 2013.

[16] J. Barros and R. I. Diego, "Analysis of harmonics in power systems using the wavelet-packet transform," *IEEE Transactions on Instrumentation and Measurement*, vol. 57, pp. 63–69, January 2008.

[17] S. Mallat, *A Wavelet Tour of Signal Processing: The Sparse Way*, 3rd ed. Academic Press, 2008.

[18] D. B. Percival and A. T. Walden, *Wavelet methods for time series analysis*, 1st ed., ser. Cambridge Series in Statistical and Probabilistic Mathematics. Cambridge University Press, 2000.

[19] D. K. Alves, F. B. Costa, R. L. de A. Ribeiro, C. M. de Sousa Neto, and T. de O. A. Rocha, "Real-time power measurement using the maximal overlap discrete wavelet-packet transform," *IEEE Transactions on Industrial Electronics*, vol. 64, pp. 3177–3187, 2017.

[20] W.-K. Yoon and M. J. Devaney, "Power measurement using the wavelet transform," *IEEE Transactions on Instrumentation and Measurement*, vol. 47, pp. 1205–1210, 1998.

[21] E. Y. Hamid, R. Mardiana, and Z.-I. Kawasaki, "Method for RMS and power measurements based on the wavelet packet transform," *IEE Proceedings - Science Measurement and Technology*, vol. 149, pp. 60–66, 2002.

[22] J. L. J. Driesen and R. J. M. Belmans, "Wavelet-based power quantification approaches," *IEEE Transactions on Instrumentation and Measurement*, vol. 52, pp. 1232–1238, 2003.

[23] W. G. Morsi and M. E. El-Hawary, "Reformulating Power Components Definitions Contained in the IEEE Standard 1459–2000 Using Discrete Wavelet Transform," *IEEE Transactions on Power Delivery*, vol. 22, pp. 1910–1916, 2007.

[24] R. d. A. Coelho and N. S. D. Brito, "Analysis of RMS Measurements Based on the Wavelet Transform," *Journal of Control, Automation and Electrical Systems*, vol. 32, pp. 1588–1602, 2021.

[25] F. B. Costa, A. Monti, and S. Paiva, "Overcurrent protection in distribution systems with distributed generation based on the real-time boundary wavelet transform," *IEEE Transactions on Power Delivery*, vol. 32, no. 1, pp. 462–473, 2017.

[26] M. M. Leal, F. B. Costa, and J. T. L. S. Campos, "Improved traditional directional protection by using the stationary wavelet transform," *International Journal of Electrical Power & Energy Systems*, vol. 105, pp. 59–69, 2019.

[27] R. d. A. Coelho and N. S. D. Brito, "A new power calculation method based on time–frequency analysis," *International Journal of Electrical Power & Energy Systems*, vol. 145, p. 108709, 2023.

[28] F. Vatansever and A. Ozdemir, "An alternative approach for calculating/measuring fundamental powers based on wavelet packet transform and its frequency sensitivity analysis," *Electrical Engineering (Archiv für Elektrotechnik)*, vol. 91, pp. 417–424, 2010.

[29] D. K. Alves, R. L. A. Ribeiro, F. B. Costa, and T. O. A. Rocha, "Real-Time Wavelet-Based Grid Impedance Estimation Method," *IEEE Transactions on Industrial Electronics*, vol. 66, no. 10, pp. 8263–8265, 2019.

[30] C. Budeanu, "Puissances reactives et fictives," *Institut Romain de l'Energie*, 1927.

[31] M. H. Bollen and I. Gu, *Signal Processing of Power Quality Disturbances*, ser. IEEE Press Series on Power Engineering. Wiley-IEEE Press, 2006.

[32] I. Daubechies, *Ten lectures on wavelets*, 1st ed., ser. CBMS-NSF regional conference series in applied mathematics 61. Society for Industrial and Applied Mathematics, 1992.

[33] W. G. Morsi and M. E. El-Hawary, "The most suitable mother wavelet for steady-state power system distorted waveforms," in *2008 Canadian Conference on Electrical and Computer Engineering*. Niagara Falls, Canada: IEEE, May 2008.

[34] É. M. Lima, R. d. A. Coelho, N. S. D. Brito, and B. A. de Souza, "High impedance fault detection method for distribution networks under non-linear conditions," *International Journal of Electrical Power & Energy Systems*, vol. 131, p. 107041, 2021.

[35] W. C. dos Santos, B. A. de Souza, N. S. D. Brito, F. B. Costa, and M. R. C. Paes, "High Impedance Faults: From Field Tests to Modeling," *Journal of Control, Automation and Electrical Systems*, vol. 24, no. 6, pp. 885–896, 2013.

[36] C. S. Burrus, R. A. Gopinath, and H. Guo, *Introduction to wavelets and wavelet transforms: a primer*, 1st ed. Prentice Hall, 1998.

[37] F. B. Costa, B. A. de Souza, and N. S. D. Brito, "Detection and classification of transient disturbances in power systems," *IEEJ Transactions on Power and Energy*, vol. 130, pp. 910–916, 2010.

[38] F. B. Costa and J. Driesen, "Assessment of voltage sag indices based on scaling and wavelet coefficient energy analysis," *IEEE Transactions on Power Delivery*, vol. 28, pp. 336–346, 2013.

[39] R. G. Stockwell, L. Mansinha, and R. P. Lowe, "Localization of the complex spectrum: the S transform," *IEEE Transactions on Signal Processing*, vol. 44, pp. 998–1001, 1996.

[40] P. K. Dash, B. K. Panigrahi, and G. Panda, "Power quality analysis using S-transform," *IEEE Transactions on Power Delivery*, vol. 18, pp. 406–411, 2003.

[41] R. Kumar, B. Singh, R. Kumar, and S. Marwaha, "Recognition of Underlying Causes of Power Quality Disturbances Using Stockwell Transform," *IEEE Transactions on Instrumentation and Measurement*, vol. 69, no. 6, pp. 2798–2807, 2020.